**VTT Technical Research Centre of Finland**

# Micromechanical and multi-scale modeling of manganese containing slag comminution in the design of energy efficient secondary raw material beneficiation processes

Lindroos, Matti; Andersson, Tom; Laukkanen, Anssi; Suarez, Laura; Kajberg, Jörgen; Jonsen, Pär; Terva, Juuso; Kallio, Marke

*Published in:*
Minerals Engineering

*DOI:*
10.1016/j.mineng.2021.106995

Published: 15/08/2021

*Document Version*
Publisher's final version

Minerals Engineering 170 (2021) 106995

Contents lists available at ScienceDirect

Minerals Engineering

journal homepage: www.elsevier.com/locate/mineng

# Micromechanical and multi-scale modeling of manganese containing slag comminution in the design of energy efficient secondary raw material beneficiation processes

Matti Lindroos [a,*], Tom Andersson [a], Anssi Laukkanen [a], Laura Suarez [b], Jörgen Kajberg [b], Pär Jonsen [b], Juuso Terva [c], Marke Kallio [c]

[a] Integrated Computational Materials Engineering, VTT Technical Research Centre of Finland Ltd., Finland
[b] Lulea University of Technology, Sweden
[c] Metso Outotec Finland Oy, Finland

ARTICLE INFO

*Keywords:*
Slag
Comminution
Micromechanics
Fracture
Crystal plasticity

ABSTRACT

Efficient separation of valuable metals from various slags is of great interest for the industry to effectively utilize valuable raw materials. Present work focuses on modeling the deformation and damage behavior of manganese containing slag materials at the microstructural level, which dictates the macroscopic material behavior and allows one to investigate possibilities to perform metal separation after comminution of the slags. The model includes finite element micromechanical description of the material behavior and slag microstructure. Computational micromodels are constructed based on direct input characterization data and statistically representative synthetic models. The damage model treats brittleness and ductility of the material together with phase specific material behavior, all relevant to comminution of the slag. Finally, a simplified jaw crusher simulation accounts for freeing materials, assisting the evaluation of empirical random breakage, all together with a microstructural particle study which is analyzed against micromechanical modeling. Crystal plasticity level simulations of surface deformation and hardening in jaw crusher are presented to couple macroscale crushing events with microscale deformation of wear parts. The work overall presents a workflow and proposes a methodology how digitalization and multi-scale material modeling can contribute to the development of efficient comminution means for hard to process secondary raw materials.

## 1. Introduction

Metallurgical industry produces slag as a co-product of metal production. Various valuable metals are embedded in the slag, making it a potential source for raw material extraction. In this view, the key asset for making metal separation from slag profitable business is to reduce the processing and extraction costs. Processing of the slag requires refinement of the larger slag pieces to suitable aggregate size for metal separation methods, given that the actual metal particles often have relatively fine size distribution within the slag. In general, transporting slag over long distances increases the costs and the energy efficiency of the processing excessively and therefore there is a need for on-site refinement methods. The slag refinement can be performed with mineral crushers, which are typically used for rock crushing.

The crushing process itself is very energy intensive, which is one major direct contributor to processing costs. Mineral liberation characteristics are mostly used in standard techniques, such as quantitative micro-structural analysis (QMA), mineralogical quantification (QEMSCAN) or chemical analysis (XRF), but experimental procedures have an economic limiting factor (Hesse et al., 2017; Leon et al., 2020). In the same context, indirect costs originate from other sources, especially from wear of the crushing equipment. Furthermore, it is essential to optimize the crushing process to be able to make use of the crushed material output most beneficially, e.g., avoid excessive generation of fine particles. The quality and performance of the comminution process is assessed by measuring the particle size distribution. The crusher choice depends strongly on the material size, desired end product and operating costs, among others (Terva et al., 2020). Macroscopic models of jaw crushers have been studied, since this kind of crushing equipment leads to higher proportion of aggregates compared to conventional

* Corresponding author. Tel. +358 40 1705601.
*E-mail address:* matti.lindroos@vtt.fi (M. Lindroos).

https://doi.org/10.1016/j.mineng.2021.106995
Received 11 July 2020; Received in revised form 22 February 2021; Accepted 30 May 2021
Available online 18 June 2021

impact machines in concrete applications (Ulsen et al., 2019). It is important to mention that regardless the type of crusher, the progressive crushing is essential in the reduction of the particle size. Then up-scaling processes are needed to optimize the whole system.

Numerical analysis procedures have become an efficient way to optimize comminution processes. Simulations of solids flow and energy transfer have been performed to get a general insight of the relation between the crushing material and the tools. Discrete Element Methods (DEM) have often been employed to describe the motion of the particles in vertical and horizontal shaft impact crushers simulations (Da Cunha et al., 2013; Djordjevic et al., 2003). The kinematics of the system are solved taking into account the interaction between the crushing elements; the total cumulative energy applied to each particle is computed to estimate the energy-size reduction and product size distribution (Djordjevic et al., 2003). (Da Cunha et al., 2013) focused on obtaining the residence time distribution and the energy collision spectra to describe the collision events and be able to extend its application to mechanistic model of comminution. By knowing information about the collision behavior within the crusher, it is also possible to get more information about the wear. The typical comminution processes used to liberate useful minerals from matrix are crushing and grinding in mills, both type of processes are complex and includes multi-physical phenomena. To include all physical events that occur in a single numerical model is today a challenging task. Most common type of numerical methods is to use particle based methods or multi-solver methods. Typical example to solve comminution problems with a multi-solver approach have been presented by (Jonsén et al., 2014; Jonsén et al., 2015; Jonsén et al., 2019; Larsson et al., 2020).

Multi-scale approaches offer a broad view to establish efficient grinding process not only from the energy consumption aspect but also with efficient benefaction of crushable media (minerals, slags) as well as with an efficient wear design point of view ((Lindroos et al., 2019; Holmberg et al., 2014; Holmberg et al., 2014)). To capture fracture behavior related to microscale phenomena, FEM-DEM coupling has been used to introduce microstructure level DEM fracture behavior together with macroscale analysis with FEM (Desrues et al., 2019). Utilization of multiscale methodology from meso-scale models up to engineering scale has shown a valuable to estimate the mechanical response of rock masses in soils (Liu et al., 2018). The key ingredient in all of these approaches is the microstructure of a material. This is much due to fact that the effect of material heterogeneities on fracture behavior can only detailed assessed with microscale, as recently discussed among others by (Golshani et al., 2006; Xie et al., 2012; Zhang et al., 2018; Sun et al., 2019; Zhou et al., 2019). For example, in terms of reusable slag materials, the microstructure of the slag defines the strength, crushability and embedded valuable phase beneficiation potential. Existing defects and given phase structure can weaken the structure to make it more easy to comminute, or vice versa, the existing complex phases structure may increase both strength and apparent ductility e.g. modify the mechanical behavior of the material. Studies of the mechanical properties of different kinds of cemented slags such as cemented mercury slag (Li et al., 2017) and fly ash/ground granulated blast furnace slag (GGBFS) geo- polymeric concrete containing (Tang et al., 2019) have been performed. (Li et al., 2017) examined specimens under uniaxial and triaxial compression tests looking for changes in the mechanical properties to derive constitutive models that describe the behavior of gravel grit mercury slag. Results of FLAC$^{3D}$ simulations of the stability of the slag showed that the behavior of the cemented slag is well captured when using a modified Duncan-Chang $E-\nu$ constitutive model. (Tang et al., 2019) describe the stress–strain behavior of geopolymer concrete with four different contents of slag under uniaxial compression tests. Results of the failure behavior and patterns show a direct effect of the content of slag on the mechanical properties, while a inverse trend on the absorption of energy.The authors agreed on the need to modify parameters in order to get a good description of the stress–strain model. These studies show the effect of the inclusion on the mechanical properties of the materials and so in the fracture behavior.

In any event, the multi-scale and microstructural perspectives provide one with ample opportunities to investigate and attempt to optimize comminution strategies. The slag materials behavior in comminution then defines the need for energy required to comminute a unit ton of material, directly depending on its heterogeneous microstructure. Furthermore, the microstructure of the slag material defines its tendency to fracture exerting certain quality end-product resembling behavior observed with rock materials.

Similarly, the microstructure of the wear parts used in the machinery defines the wear life of a given material (Lindroos et al., 2019; Lindroos et al., 2018; Lindroos et al., 2018; Lindroos et al., 2015). To estimate the microstructural level deformation and resulting wear behavior, a coupling of macroscale machinery and its loadings to microscale material behavior must be established. Besides increasing the understanding in the comminution process, a well defined modeling and experimental workflow generates new possibilities to affect process energy efficiency with optimized use of machinery, designed selective comminution on end-product quality, and tailor wear resistant solutions with respect to a specific medium being comminuted.

Current work focuses in providing a multi-scale workflow to estimate slag material mechanical behavior from microstructural level up to comminution by a jaw crusher, which is modeled in a macroscopic context. The methodology is valuable in providing the necessary material parametrization for fracture models needed in macroscale simulations that now originate and consist of information from the slag microstructure. The modeling framework outcomes are aimed to be used as a part of optimizing energy efficiency of slag material crushing and to understand the force levels existing during comminution. The balance in optimizing usage of a mineral crusher in the process to achieve benefits of selective comminution, also inflicts moderate to severe loading to equipment surfaces that undergo wear and may increase costs of use. For complex slag material microstructures specifically, analyses are made to benchmark feasibility of a microstructurally informed homogenization method with a direct microstructure based heterogeneous approach. Various characterization techniques are utilized to establish the information necessary for multi-scale simulation models. To introduce a preliminary link to crusher material deformation and ultimately wear, the second part of the work focuses on providing a simplified coupling of macroscale mineral crushing with mesoscale material behavior (plasticity) of wear parts (jaw material) ultimately relevant for material wear behavior and prediction of lifetime of wear parts. Altogether the work provides a view to multi-scale modeling of energy efficient secondary raw material beneficiation processes. Furthermore, the roles of different modeling approaches are discussed with respect to establishing viable and exploitable multi-scale modeling strategies.

## 2. Materials and methods

### 2.1. Modeling framework

The challenge in modeling of the comminution process is that it is inherently multiscale, even if we focus solely on the crushing stage. This results from the simple fact that the most significant characteristics responsible for the damage and fracture response, with respect to the material scale ultimately influencing the crushing process, are the microstructural and micromechanical behavior. The interesting performance characteristics for crushers relate to the efficiency, final product quality and equipment lifetime, i.e., wear. These are both, macroscopic (”product scale”) and microstructural (i.e., lifetime of wear parts when treated micromechanically) features. Thus, in order to tackle the problem ultimately holistically a multiscale concept becomes a necessity, and for current work, the development of such a toolset and analysis methodology has been following the concept presented in Fig. 1. The proposed concept the results of which are partially covered in current paper consists of three main elements including their primary functionalities:

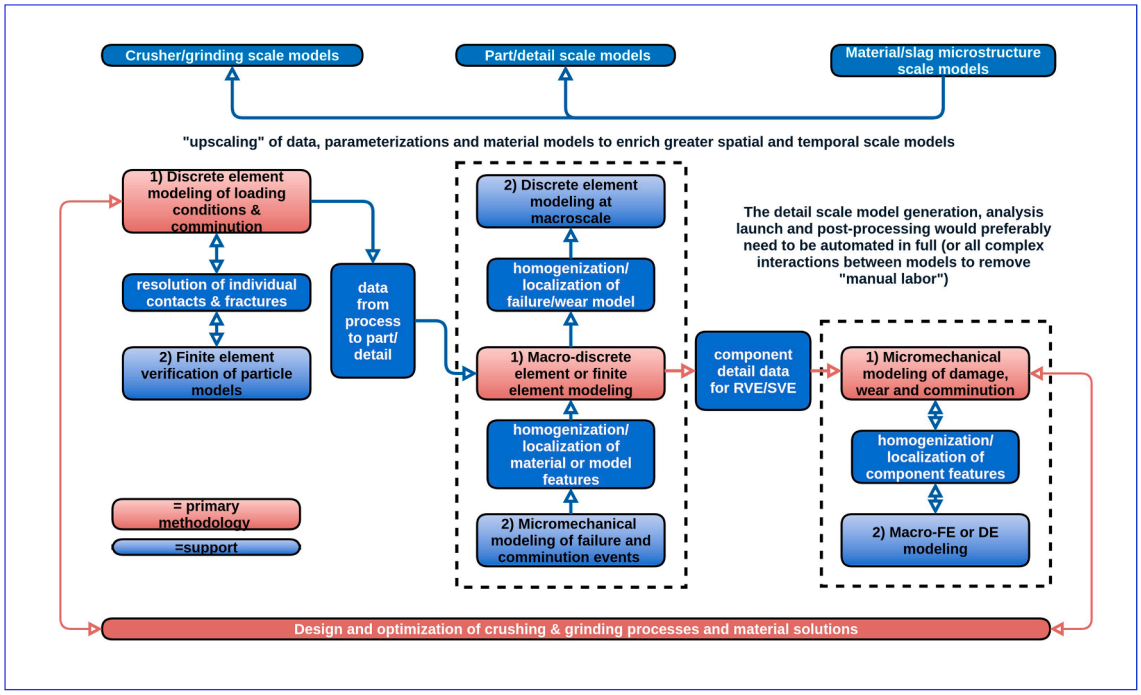


**Fig. 1.** Concept of micromechanically informed modeling of comminution.

- Discrete element modeling for process and crusher scale modeling, resolution of material flow and interaction with the component scale geometry.
- Macroscale modeling of particle to crusher contact at the scale of the comminution process, i.e., resolution of the contact responsible for the fracture and refinement of the processed material.
- Microscale modeling of the fracture process with the product being processed, i.e., linkage of the material microstructural scale and its characteristics to the comminution process.

With these three interacting approaches it can be argued that the crushing process, crusher and material scales can be linked. Thus, the objective of investigating how to efficiently refine a particular raw material can be addressed systematically with the aid of modeling. Regarding the linkages, two approaches are utilized within the present scheme and are briefly included also in Fig. 1. Firstly, larger spatial scale analyses can yield data to smaller scale representative volume elements (RVEs). For example, from a DEM analysis the individual particle contacts can be extracted from a particular locale (such as a crusher jaw) and resolved in more detail with a smaller scale model. This smaller scale model adds information, for example, with respect to effects of particle geometry or microstructure on the respective process and can produce, for example, more complex fracture behavior and track the propagation of cracks within the microstructure. Secondly, a simpler approach using localization and homogenization between scales can be utilized. In this scale statistical and mean field data is transferred across the scales which can, for example, in contact resolution, lessen the computational cost significantly while for many cases the accuracy is still sufficient.

The primary implementations of the individual tools at present utilize high-performance computing (HPC), the following developments will initiate taking steps towards, e.g., surrogate models. In addition to the production process development, the ultimate objective is to provide a novel simulation tool which can be used for planning and optimization of the respective processes for different secondary raw materials. The simulation tool is focused on describing the whole refining process starting from ”raw” slag by introducing respective modelling capabilities as a customization of the workflow. The simulation tool can predict the size distribution and morphology of the end product after crushing steps in the process sequence. In general, micromechanical models aim to parametrize macroscale finite element slag deformation and fracture models, that can be used to establish benchmarking among different crushing/refinement methods. The macroscopic models provide a direct link to energy efficiency when coupled to micromechanically informed fracture models of slags. The slag composition varies significantly, and it is highly expected to lead to different energy absorption behaviors. The linking between microscale and macroscale fracture models is also required to define a range of parameters for DEM models as a function of slag composition. Also, the energy need for the whole crushing process is a target to be better evaluated. This provides one with the capability to develop and optimize comminution processes and improve their efficiency for the beneficiation of difficult to process raw materials.

### 2.2. Slag material

Fig. (2a) shows manganese containing slag particles crushed from the residual slag generated by a smelting process. The larger slag pieces contain both relatively sharp and rounded slag particles that are similar to many rock materials appearing in nature. The extraction of valuable manganese from the slag requires comminution of the slag particles to a sufficient size range for robust extraction.

The investigated slag material contains several phases, which are identifiable in Fig. (2b-c). The composition of the manganese containing inclusions, appearing generally brighter spots in the images, varies between three main compositions of MnFeSi, SiMnFe and small MnS droplets. The matrix consists three dominant phases, amorphous CaSiAlMgMnO, crystalline SiCaAlMgO, and amorphous/crystalline mixture phase SiAlCaMnMgKO. An average matrix volume fraction of the dominant phases is 89 % and average manganese inclusion volume fraction is approximately 8.8 %, while the remaining compositions are listed in Table 1. The presently investigated slag material also contains notable amount of small and large pores.

Kuru granite is used as a reference material in the simulations to address the crushability and benchmarking of the investigated slag material, for example, in comparing model parameterizations. Kuru granite is a high strength rock material (Hokka et al., 2016; Fourmeau

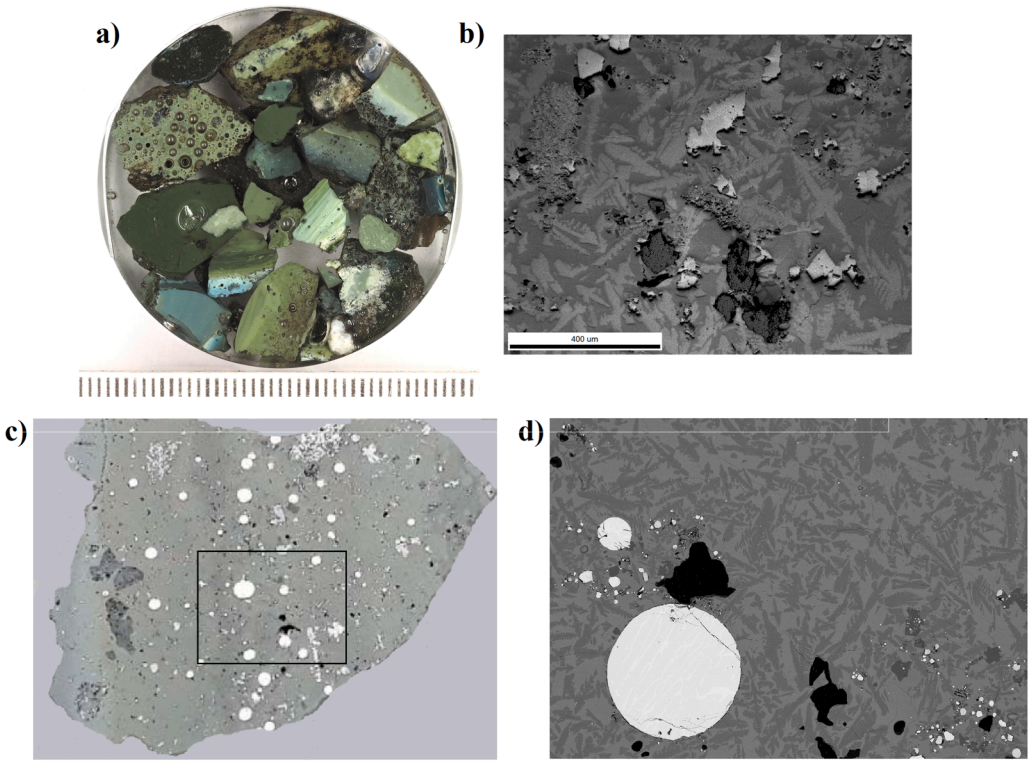


**Fig. 2.** a),c) Manganese slag particles, (b), (d) SEM micrographs of the slag microstructure (Apazablanco et al., 2020).

**Table 1**
Phase fractions identified from slag samples (Apazablanco et al., 2020).

| Mineral | SE-1-wt% | SE-2-wt% | SE-3-wt% | SE-4-wt% | SE-5-wt% | Feed-Wt% |
|---|---|---|---|---|---|---|
| CaSiAlMgMnO | 98.61 | 64.17 | 0.68 | 86.02 | 40.73 | 58.04 |
| SiCaAlMgO | 0.03 | 6.42 | 76.10 | 11.20 | 26.49 | 24.05 |
| SiCaAlMgKMn | 0.00 | 0.19 | 0.00 | 0.03 | 0.14 | 0.07 |
| SiAlCaMnMgKO | 0.02 | 12.67 | 20.86 | 1.51 | 0.45 | 7.10 |
| MgSiMnO | 0.00 | 0.00 | 0.41 | 0.00 | 0.00 | 0.08 |
| Si | 0.20 | 4.44 | 0.000 | 0.25 | 1.36 | 1.25 |
| SiO | 0.00 | 0.67 | 0.00 | 0.00 | 0.00 | 0.13 |
| AlO | 0.00 | 0.01 | 0.00 | 0.00 | 0.00 | 0.00 |
| Ti | 0.00 | 0.01 | 0.01 | 0.00 | 0.00 | 0.00 |
| MnSiFe1 | 0.34 | 7.92 | 0.00 | 0.47 | 22.92 | 6.33 |
| MnSiFe2 | 0.63 | 3.20 | 0.02 | 0.44 | 2.70 | 1.40 |
| MnS | 0.00 | 0.21 | 1.92 | 0.05 | 0.00 | 0.44 |
| SiMnFe | 0.16 | 0.09 | 0.00 | 0.01 | 5.20 | 1.09 |
| SiFeMn | 0.00 | 0.00 | 0.00 | 0.00 | 0.00 | 0.00 |

et al., 2017) and also its comminution is an energy consuming process. Furthermore, Kuru granite has been known to cause severe wear when it is involved in abrasive and erosive contacts with wear resistant engineering materials (Lindroos et al., 2015).

### 2.3. Micromechanical model of slag material

The material modeling is performed with an anisotropic strength and failure model. The model is a variant of the original Johnson-Holmquist II (JH-II) material model used for various brittle materials (Johnson and Holmquist, 1994). It is assumed that the brittle slag material matrix phases deform and fail similarly to many rock materials. Tensile-compression asymmetry is highly relevant to material's crushing process because the strength of the material is taken to increase with respect to increasing hydrostatic pressure (e.g., confinement pressure at macroscale). Mechanical experiments were performed for the slag material to establish a view to tensile-compression anisotropy and the results are discussed in more detail in Section 3.1.

The strength of the slag material is given as a function of unconfined uniaxial compressive strength and its tensile strength. In addition, the material is assumed to have a certain strain rate dependency, accompanying pressure dependency. For example, Kuru granite has been observed to have significant strain rate dependency (Sakala et al., 2017; Hokka et al., 2016). This is highly relevant aspect in terms of the material failure prediction capability because the strain rates in high performance crushing are expected to be in the dynamic range, which affects the material strengthening in both compression and tensile stress states. The material's flow stress $\sigma^{str}$ is given by:

$$\sigma^{str} = A(P^* + T^*(1-D))^N\left(1+\frac{\dot{\epsilon}}{\dot{\epsilon_0}}\right)^C \; with\, P^* = \frac{P}{\sigma_{UCS}}\; T^* = \frac{T_{max}}{\sigma_{UCS}} \tag{1}$$

where $A$ and $N$ are material strength parameters, $C$ is a strain rate parameter, $\dot{\epsilon}$ is the strain rate, $\dot{\epsilon}_0$ is the reference strain rate, and $D$ is the accumulated damage variable. Hydrostatic pressure related variables $P$ (compression) and $T$ (tension) are scaled with uniaxial compressive strength $\sigma_{UCS}$. Later uniaxial compressive strength is denoted as UCS. The original JH-II distinctly separates the strength behavior for fully intact material and partially fractured materials, however, defining such material parameters is a difficult task on a phase specific basis. Therefore, the present work utilizes only one strength parametrization with direct coupling to damage that mimics the intact and fracture material behavior through one variable, as was also performed in Ref. (Fourmeau et al., 2017). When the material is partially cracked and contains damage, tensile and compressive strengths of the material are reduced accordingly. It is worth noting that material has strength in compacted condition, i.e., when the hydrostatic pressure is negative. This choice in the material model provokes that small particles can be compacted and the material can carry load in compression in spite of large crack density.

The yield of the material is taken to follow von Mises plasticity driven by equivalent stress, and the flow rule reads:

$$\sigma^{eqv} - \sigma^{str}\cdot\sigma_{UCS} \leqslant 0 \tag{2}$$

Damage variable is a function of plastic strain and its relation to incremental fracture strain of the material.

$$D = \int_{t=0}^{t} \frac{\Delta \epsilon^p}{\epsilon_f^p} dt \quad (3)$$

where $\Delta \epsilon^p$ is the plastic strain increment and $\epsilon_f^p$ is the fracture strain, which depends on the hydrostatic pressure and the tensile strength.

$$\epsilon_f^p = D_1 (P^* + T^*)^{D_2} \quad (4)$$

where $D_1$ and $D_2$ are damage variables controlling the increase of fracture strain. Pressure of the material is defined by three material parameters. However, the higher order terms introduced by $K_2$ and $K_3$ are set zero in the present context for simplicity.

$$P = K_1 \mu + K_2 \mu^2 + K_3 \mu^3 \quad (5)$$

Each matrix phase has different material parametrization. The manganese containing intermetallic inclusions are treated as linearly elastic in the present case for simplicity. It is should be noted that the inclusions may also crack during deformation in some cases.

The simulation in this work were performed with Abaqus finite element software using explicit solver with a VUMAT material subroutine.

## 3. Results

### 3.1. Material model parametrization

Indentation hardness and $K_{IC}$ fracture toughness values were measured for the dominant phases. Measured microhardness and fracture toughness values were utilized in the estimation of phase specific material parameters. For the estimation of tensile strength of each phase, an empirical relation $T = 6.88 K_{IC}$ was used as a starting point (Zhang, 2002; Feng et al., 2019) for the calibration and then further adjusted with simulations. Table 2 lists the final used phase specific material model parameters for slag, and macroscopic parameters for granite. The material parameters for granite resemble the ones identified in Ref. (Fourmeau et al., 2017) with some variations. Fracture toughness value was linked to fracture susceptibility by adjusting damage parameters $D_1$ and $D_2$ to correlate with $K_{IC}$ difference between phases. No direct physical meaning was established and their correlation is only relative to each other. Microhardness values were used to scale uniaxial compressive strength of the phases. The measured macroscopic point load hardness was selected as baseline for the correlation. The phase specific values were further calibrated in hardness related order to achieve similar UCS for the homogenized structure as for experimentally measured UCS values. Many studies address the relationship between indentation hardness and UCS, however, the goodness of the correlation varies, e.g., Refs. (Kahraman et al., 2012; Zavacky et al., 2017). Therefore, the choice of hardness to UCS correlation function is not necessarily unique. Granite rock parameters were used as a reference for scaling of slag material parameters. In the absence of pressure-dependent and strain rate dependent parameters for slag phases, the parameters were chosen to in accordance with granite parameters to provide sufficient strain rate dependency. Damage parameters were set lower than for granite, assuming more pronounced brittle behavior.

Unconfined uniaxial compression test and Brazilian disc tests were performed to approximate UCS and $T_{max}$ at macroscale for the slag particles having a composite microstructure. It was observed that the uniaxial compressive strength varies greatly for the material, depending on the composition quality of the used samples. Furthermore, point load test and uniaxial compression tests suggest different UCS values for the material, partly because of pre-existing defect density in the cylindrical samples. The Brazilian disc test samples included notable amount of pores and pre-cracks. Therefore, the measured tensile strength (value circa 1/20 of UCS) of the slag material can be considered as an low-end estimate in compared to more conventional 1/10 tensile strength value of the uniaxial compressive strength a rock material.

**Table 2**
Phase specific material model parameters used in simulations and experimental data on Mn-slag and Kuru-granite (Mn-slag results from Apazablanco et al. (2020)).

| Phase | SiCaAlMgO | CaSiAlMgMnO | FeMnSi | Granite |
|---|---|---|---|---|
| Bulk modulus [GPa] ($K_1$) | 40.0 | 40.0 | 100.0 | 54.0 |
| Shear modulus [GPa] ($G$) | 20.0 | 20.0 | 60.0 | 31.0 |
| Compressive strength [MPa] ($UCS$) | 164.0 | 140.0 | - | 235.0 |
| Tensile strength [MPa] ($T$) | 16.4 | 13.4 | - | 18.0 |
| Strength parameter ($A$) | 1.4–2.2 | 1.4–2.2 | - | 2.23 |
| Strength exponent ($N$) | 0.68 | 0.68 | - | 0.68 |
| Strain rate exponent ($C$) | 0.005 | 0.005 | - | 0.0094 |
| Reference strain rate ($\dot{\epsilon}_0$) | $10^{-5}$ | $10^{-5}$ | - | $10^{-5}$ |
| Damage parameter ($D_1$) | 0.0324 | 0.0324 | - | 0.077 |
| Damage exponent ($D_2$) | 0.25 | 0.25 | - | 0.46 |
| **Measured microscale values** | | | | |
| Microhardness [$HV$] | 925 ± 35 | 720 ± 40 | 1000 ± 50 | - |
| Fracture toughness [$MPA{\cdot}m^{1/2}$] | 1.0 ± 0.4 | 0.9 ± 0.3 | 1.7 ± 0.5 | - |
| **Material strength** | **Mn-Slag** | **Kuru-Granite** | | |
| Compressive strength (UCS) [MPa] | 162.3** ; 123.2* | 235 (Hokka et al., 2016) | | |
| Tensile strength ($T_{max}$) [MPa] | 3.7 –5.4* * * | 8–14.25 ( Mardoukhi et al., 2017) | | |
| Notation<br>* Cylindrical samples<br>*** Point load test<br>**** Discs with large pores and pre-cracks | | | | |

### 3.2. Mesoscale models

Mesoscale models and micromechanical models were established based on the microscopic characterization. Fig. 3a illustrates a mesoscale model with matrix and inclusion phases, by utilizing the numerical means presented in more detail in Holmberg et al. (2014),Holmberg et al. (2014), Laukkanen et al. (2016). The matrix material (red) was treated as one material with averaged properties of the matrix phases, while the inclusions (blue) were elastic. The interface mixed regions (grey) were assigned to have 10–20 % lower strength parameters based on visible porosity and openness of the boundaries (UCS and TS).

Compression simulations were performed on the mesoscale microstructure to analyze the effect of strength parameters to homogenized uniaxial strength of the microstructure. Fig. 3b,c show the equivalent stress and damage maps at the early stages of damage evolution and at the end of the simulation. Stress concentrations are observed around the manganese containing inclusions and the interface regions experiencing high stresses initiate the damage. Tensile fracture is the dominant failure

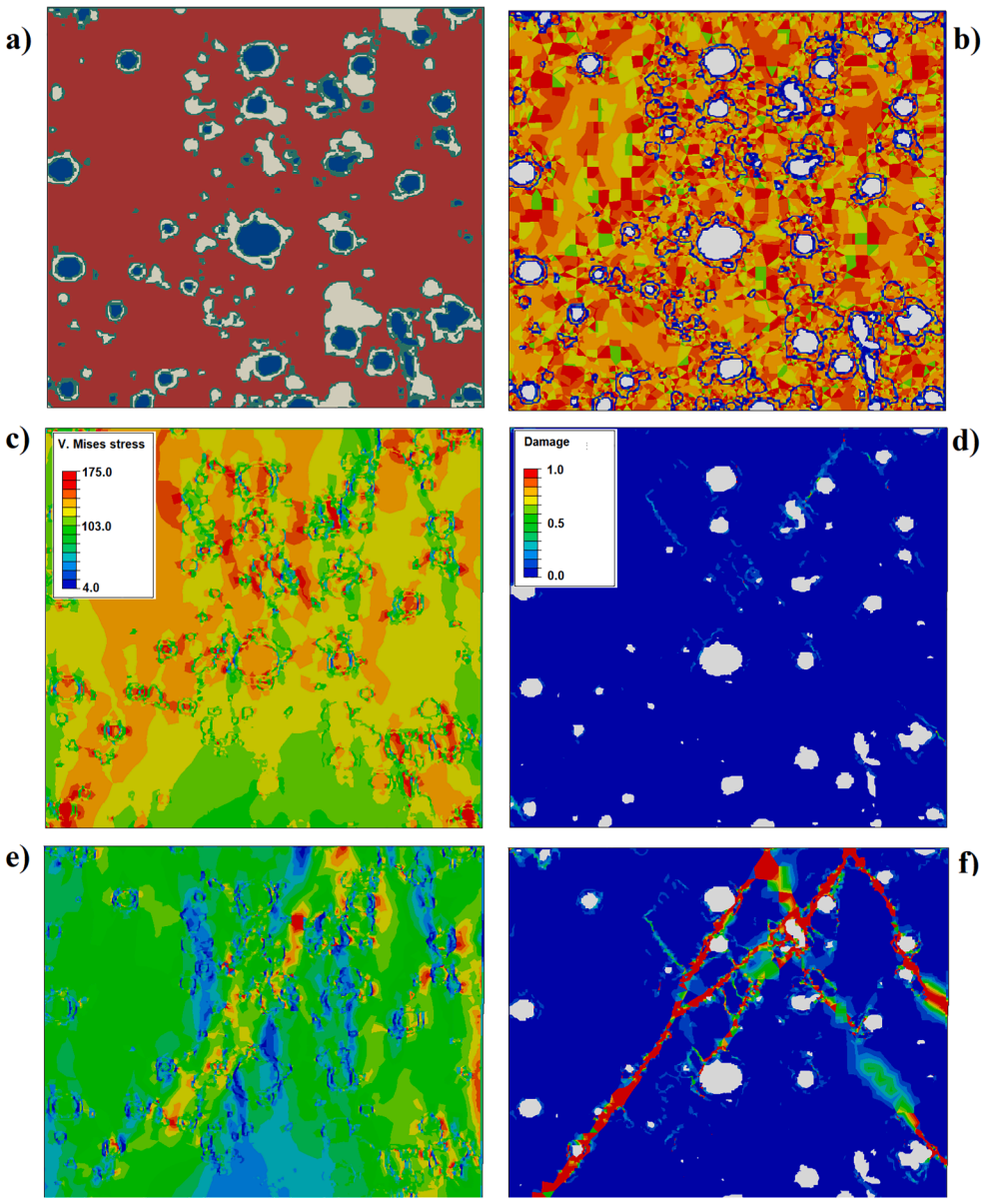


**Fig. 3.** a) Computational microstructure, b) tensile strength map with homogenized matrix. Equivalent stress and corresponding damage field c)-d) during early stages of damage evolution, e)-f) at failure. Loading direction is aligned to vertical axis in compression. Domain size is ca. 2200 $\mu m$ and mesh size varies between 20–80 $\mu m$.

mechanism, however, the crack network includes contributions from shear damage in the regions with compressive stresses.

Fig. 4 shows the effect of strength parameter $A$, while UCS and TS parameters were kept constant during the simulations. The stress–strain curves are plotted for the investigated microstructure by averaging stress and strain values over the aggregate. The results indicate that a feasible range for the material parameter $A$ is 1.3–1.8, as the experimentally measured UCS values for the slag material range in 123–162 MPa depending on the testing method and slag heterogeneity.

The effect of matrix microstructure is also relevant in the parametrization process. Fig. 5a shows another type of microstructure based model with discretized two phase matrix. The model aims to elucidate the effectiveness of matrix hetergoneities arising in the simulations. Different material properties were assigned to SiCaAlMgO and CaSiAlMgMnO phases, which are considered the dominant compositions forming the lamellar like microstructure. In addition, pores were included in the computations to introduce the observed weakened structure. The uniaxial compression simulation shows that damage grows rapidly in the matrix and interface regions. It is clear that the discretized matrix microstructure has a role in the damage propagation process. More heterogenous stress state is formed if compared to the homogenized matrix approach in Fig. 3. The local stress state affects the susceptibility to damage, i.e., cracks grow and arrest at apparent microstructure features, which is expected for the needle-like dendritic structure.

The stress–strain curve of the heterogeneous matrix approach in Fig. 4 show that the strength parameter 1.4 can overestimate the macroscale UCS values of the slag material. Damage parameters have an effect on the plasticity-damage part of the stress–strain curve, i.e., after yield up to fracture. However, the fracture tendency and the strength is ultimately defined by the dominant material parameters that are the strength fitting parameters $A$ and $N$ as well as phase specific UCS and TS values.

To this extent, the plasticity-damage controlled regime is mostly operated within a narrow scope in the materials strength for quasi-brittle materials, i.e,. after plasticity, the actual plasticity-damage

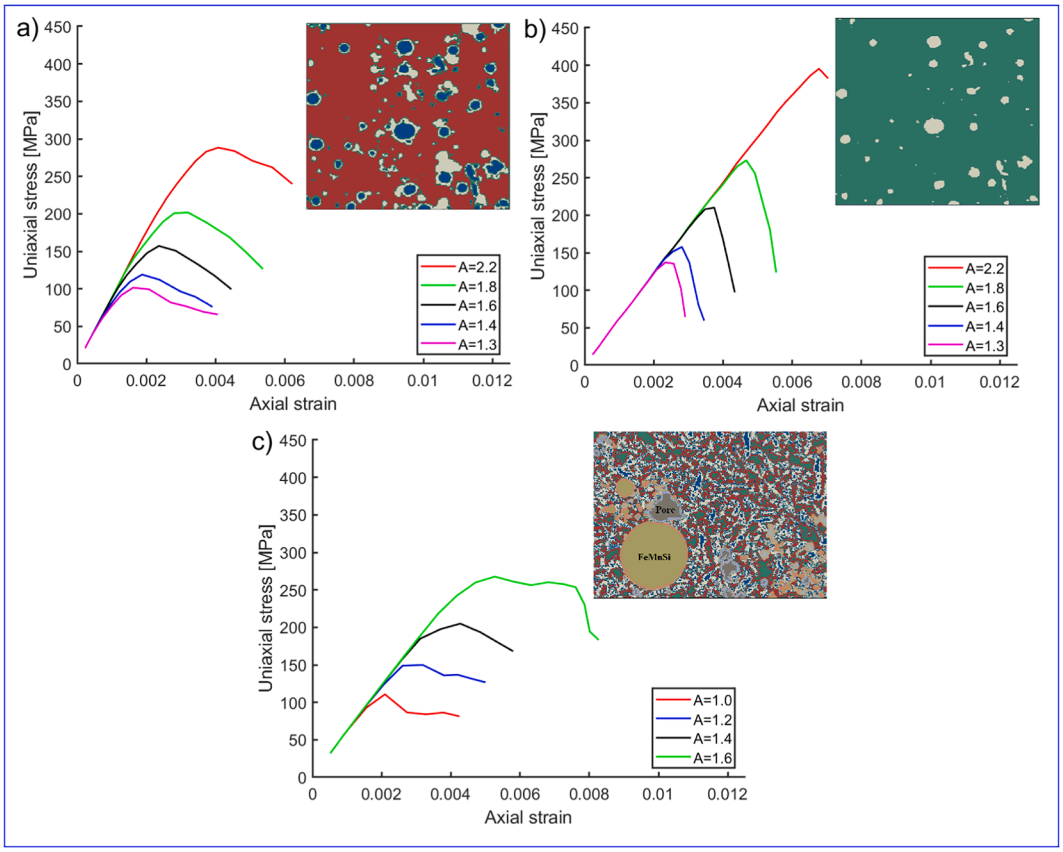


**Fig. 4.** Uniaxial compression simulation of meso-scale microstructures with the effect of strength parameter *A* for a) interface heterogeneous model, b) ideal two-phase model, c) heterogeneous microstructure model.

operated range is small before maximum stress and following stress drop are observed. Thus, the uncertainty related damage parametrization has some effect on the homogenized UCS outcome of the microstructure. However, the choice of damage parameters is in lesser role than general phase specific strength parameters. In this view, a reasonable estimation of these parameters can suffice to yield first approximation of the material crushability and energy consumption in comminution. Essentially, however, it should be noted that the damage parameter and crack evolution in the microstructure becomes more relevant when predicting the end product size and shape distributions after crushing because of the crack network propensity in a slag particle. This aspect, however, is beyond the scope of this work. Present work focuses on the multi-scale aspects of the slag modeling. As a compromise of the two modeling approaches, the value 1.4 is retained for *A* in the following simulations, in addition to the parameters listed in Table 2.

### 3.3. Jaw crusher

Simplified single action crushing simulations were performed to analyze the effectiveness of different multi-scale approaches. In the first case, an arbitrary shaped rock-like particle is assigned to have different amount of manganese inclusions and matrix by choosing a certain volume fraction of the elements to be FeMnSi material. The second case analyzes discretized inclusion phase, two matrix phases, and pores in a synthetically generated slag particle. Fig. 6a illustrates the initial simulation setup with two jaws and one rock/slag particle. One of the jaws is fixed stationary and the other jaw is linearly displaced towards the stationary jaw to imitate crushing sequence. The simulation is continued until the mineral particle is fractured. Small amount of pressure is subjected on the top part of the rock/slag particle to hold the particle in between the jaws when the contact is encountered.

Two simulation cases were investigated. The first crushed medium is imposed as granite reference material and the second is a two-phase slag material with single element sized inclusions and a surrounding matrix phase. The reference granite material is introduced with a 30 % variations in the local tensile strength properties, which is displayed in Fig. 6b. Fig. 6c shows the range in manganese-inclusion content in red colour. The volume fraction of FeMnSi inclusions was varied from five to fifteen percent.

Fig. 7 shows the contact forces between the stationary jaw and rock/slag particle. Early part of the curve accounts for the first contact force that translates and finally compresses the particle against the stationary jaw. A following sudden decrease occurs due to initial contact zone cracking of the particles. The primary fracture cycle occurs at a later stage, while increasing to the maximum observed force values for granite and two slag cases. No distinctive difference was observed between slags containing 5 % and 15 % volume fraction of FeMnSi particles. This behavior indicates that the chosen parametrization for the matrix phase is more important role than the secondary phase, i.e., FeMnSi in this case. The absolute value of resultant force is slightly higher for slag than granite in the present simulation case. In contrast, shear forces (Y and Z directions) are generally larger for granite and more distinctive multistage cracking behavior is also observed for granite. It was observed that slag material develops first cracks in the contact zone and individual crack regimes begin to appear, spanning the cracking process longer than for granite. Finally in both of the studied cases, a sudden collapse is observed to follow the peak force due to full developed crack networks in the particle.

Fig. 8 presents two virtual slag particles with discretized phases. The slag particles were crushed in the jaw crushing simulation and compared with granite using the same method. The referencing to granite was established by allocating granite material parameters to all phases, i.e.,

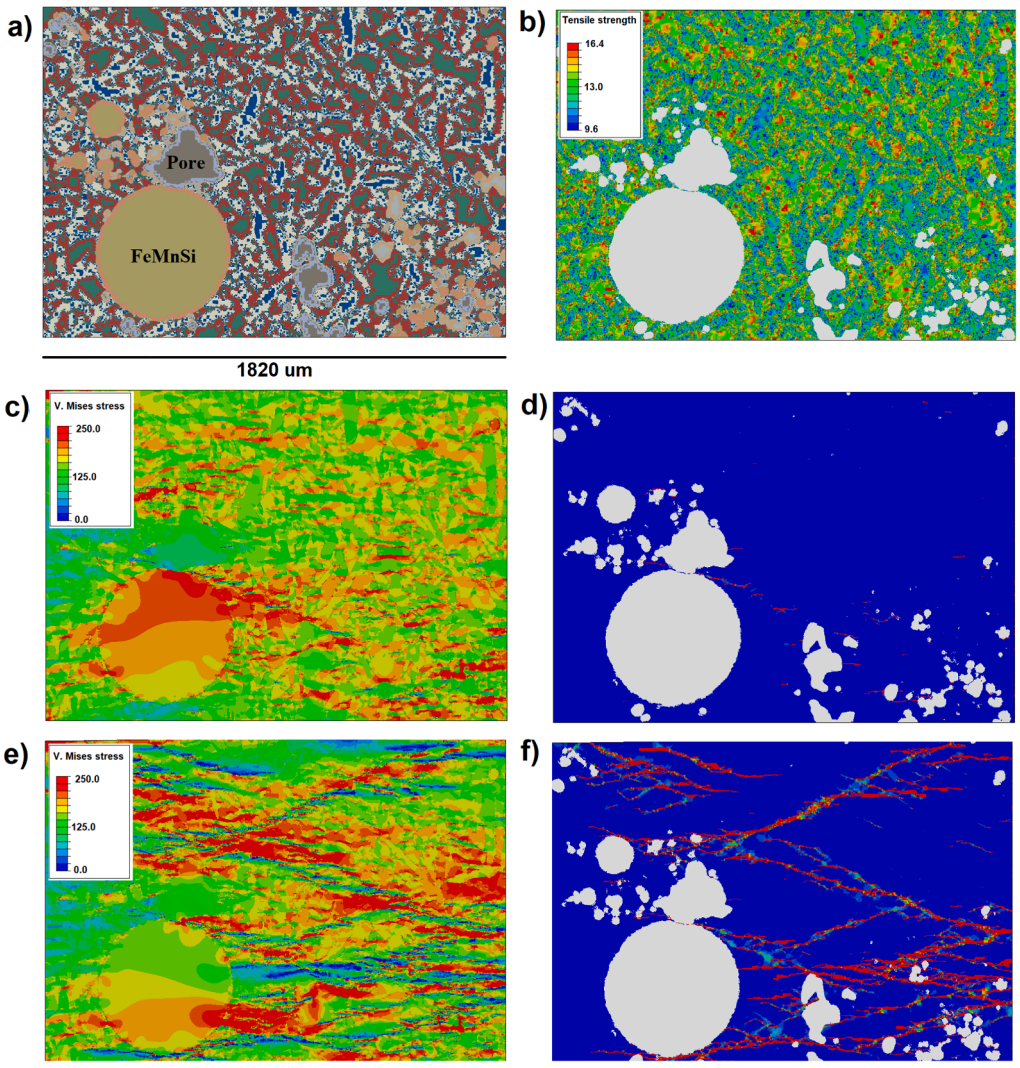


**Fig. 5.** a) Computational heterogeneous microstructure, b) tensile strength map heterogeneous matrix. Equivalent stress and corresponding damage field c)-d) during early stages of damage evolution, e)-f) at failure. Loading direction is aligned to horizontal axis in compression. Mesh size is generally between 2–10 $\mu m$..

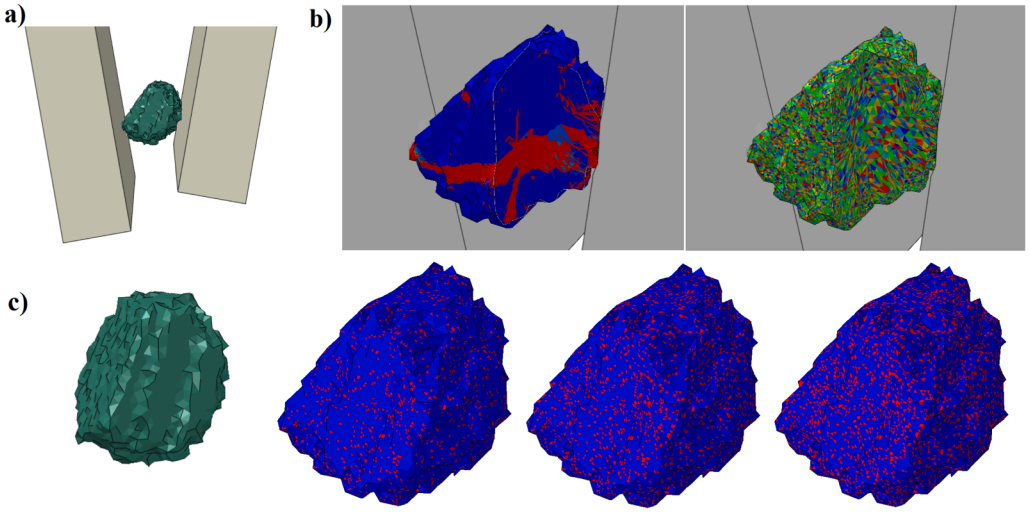


**Fig. 6.** a) Contact assembly of the jaw crushing simulation, b) damage field during crushing and a mapping of tensile strength in granite, c) feed rock or slag piece for the simulations and mappings of FeMnSi-inclusions in the mesh with 5, 10 and 15 percent volume fraction of inclusions.

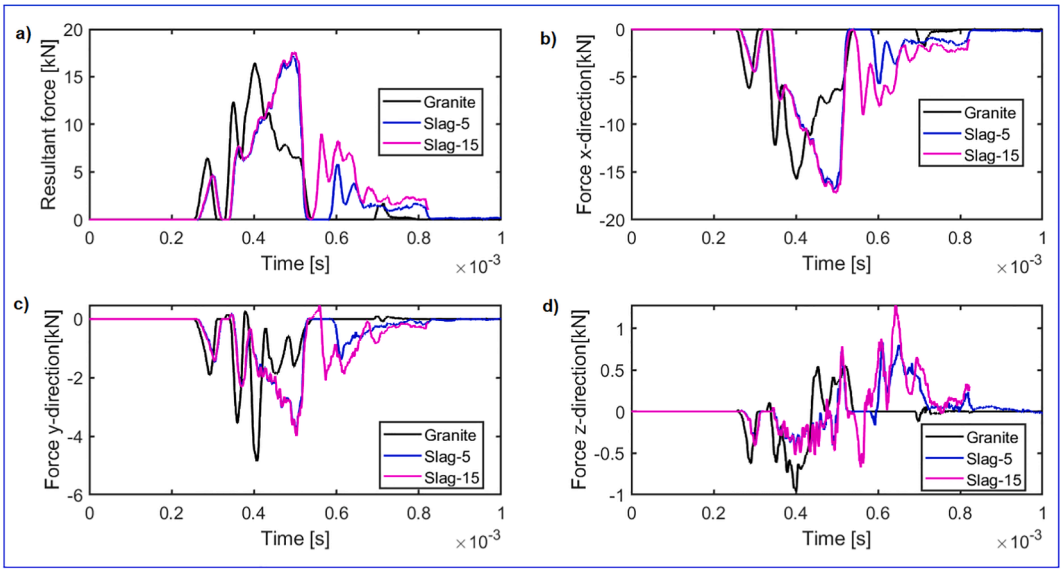


**Fig. 7.** Contact forces in the jaw crushing simulation. a) Resultant forces for granite and different slags with variations in FeMnSi inclusion volume fraction, and b)-d) individual force components.

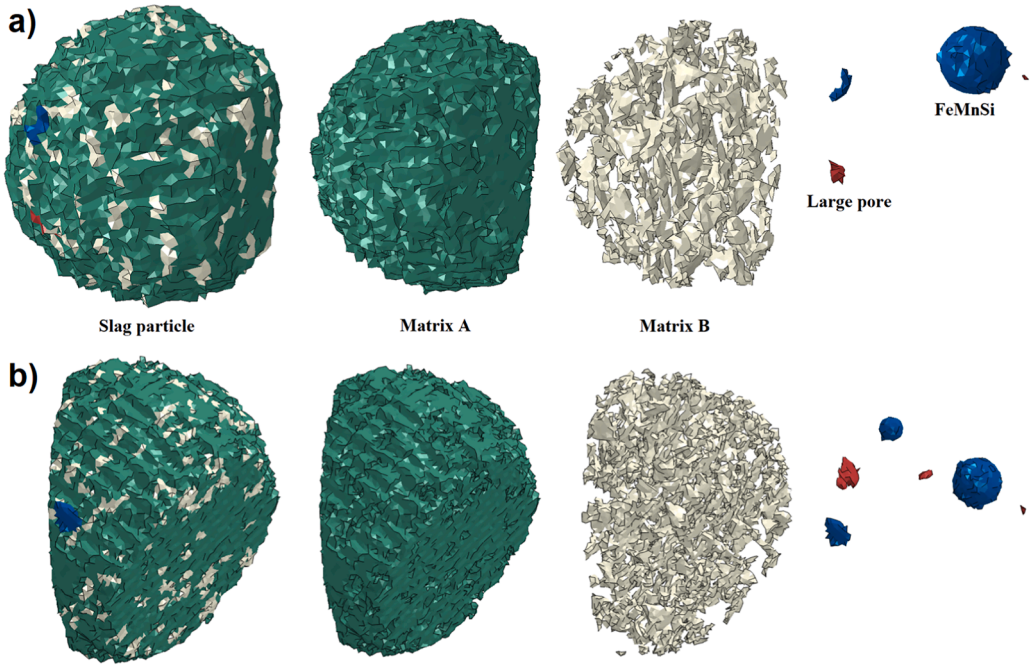


**Fig. 8.** Two synthetic slag particles with two matrix phases and FeMnSi-inclusions and one large pore defects.

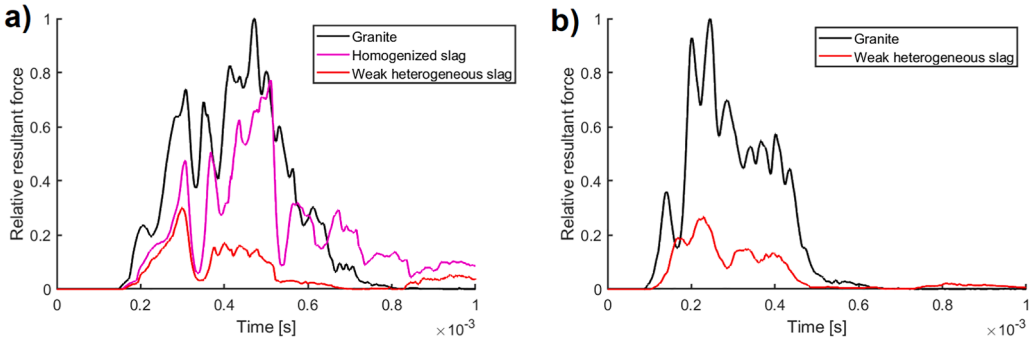


**Fig. 9.** Relative resultant crushing force for granite, homogenized slag and explicit slag microstructure. Scaling is performed with respect to granite.

removing distinction between phases and using one phase only for granite. Similarly, in the case of homogenized slag, the properties were assigned to the slag particle by omitting four phase structure. The material is assigned with 10 % element based volume fraction of FeMnSi-inclusion material with a similar approach shown in Fig. 6c. The geometry and finite element discretization of the slag particle remains unchanged and only the internal material properties vary between the cases.

Simulations show that the discretized heterogeneous slag particle is notably weaker than homogenized slag particle. Only about 40 % of the maximum force of homogenized particle is reached. This results partially from the increased stress heterogeneity in among the two distinct matrix phases and the manganese-inclusion. In the present cases, the pore had negligible effect on the fracture behavior as the force curves of pore and non-pore slag particle were almost identical. The pores were located in the less stressed zone in the slag particle. The force curves again show two main amplitudes of crushing force that is generated by the initial and primary contact and failure of the crushed particle. The initial contact generates damage mainly in the zones near particle-jaw contact, while the primary crushing phase deteriorates existing residual strength of the partially damaged particle and crushing is finalized in the simulation.

Fig. 10 shows loaded and partially damaged heterogeneous and homogeneous slag particles during crushing sequence. The heterogeneous slag particle has higher tendency to develop clear crack paths and scarce damage networks that leads to overall failure, i.e., the cracks are more local in nature. The fracture occurring in the homogenized slag particle with a large number of small inclusion zones resembles a material that is strengthened with hard particles. Due to relatively dense inclusion distribution, the straight-through cracks are less probable to develop in the simulated case and the inclusions act as hardening phase in the material arresting advancing cracks. The increased stress threshold of the particle then increases the materials nominal strength, that observed as the increased maximum force peak in the force curves in compared to the heterogeneous case. The particle finally cracks under severe stress state, while developing dense crack networks around the hardening inclusions, finalizing the crushing sequence. In terms of mimicing the microstructure of the presently investigated slag material, the full explicit introduction of four phases is justified due to more accurate description of FeMnSi-inclusions and their precipitation.

### 3.4. Micromechanical approach on jaw material deformation

One part of the multi-scale modeling workflow of energy efficient mineral and slag comminution are the wear challenges related to materials withstanding the crushing loads. Premature and localized wear of the jaws can reduce the overall efficiency of the crushing process by causing increased energy consumption and decrease the quality of comminuted end-products. The following aims to incorporate jaw material micromechanics into the presently proposed multi-scale workflow, that can be used to address and control wear phenomena in mineral and slag comminution.

The deformation behavior at microstructure scale was simulated with a crystal plasticity model. In-depth derivation and verification of the crystal plasticity model focused for Hadfield steels has been performed in Refs. (Lindroos et al., 2018; Lindroos et al., 2018) for various loading conditions. This model framework together with the model parametrization for Hadfield steel is used in the following simulations. The model describes plastic deformation in the material by dislocation slip and deformation twinning. The material's extraordinary hardening capability combined with good ductility results from the interactions of dislocations and deformation twins, capable of increasing the material's surface hardness to 2–3 times of the initial as-cast hardness.

A length-scale issue rises from the origin of material failure in the microscopic scale and its actual realization in the macroscale crushers. Deformation, hardening and failure processes are all local grain and grain to grain interaction dependent phenomena, which leads to a need to describe a material microstructure at a sufficient accuracy to be able to capture the essential causalities. The actual contact area of mineral or slag particles interacting with the jaws is not necessarily very large. Therefore, the contact pressure and sliding motion of the particles cause severe stresses to the surface of the jaws. Wear is intuitively expected to result most significantly due to abrasive contact causing ploughing and cutting assisted by fatigue, which has also been observed in previous

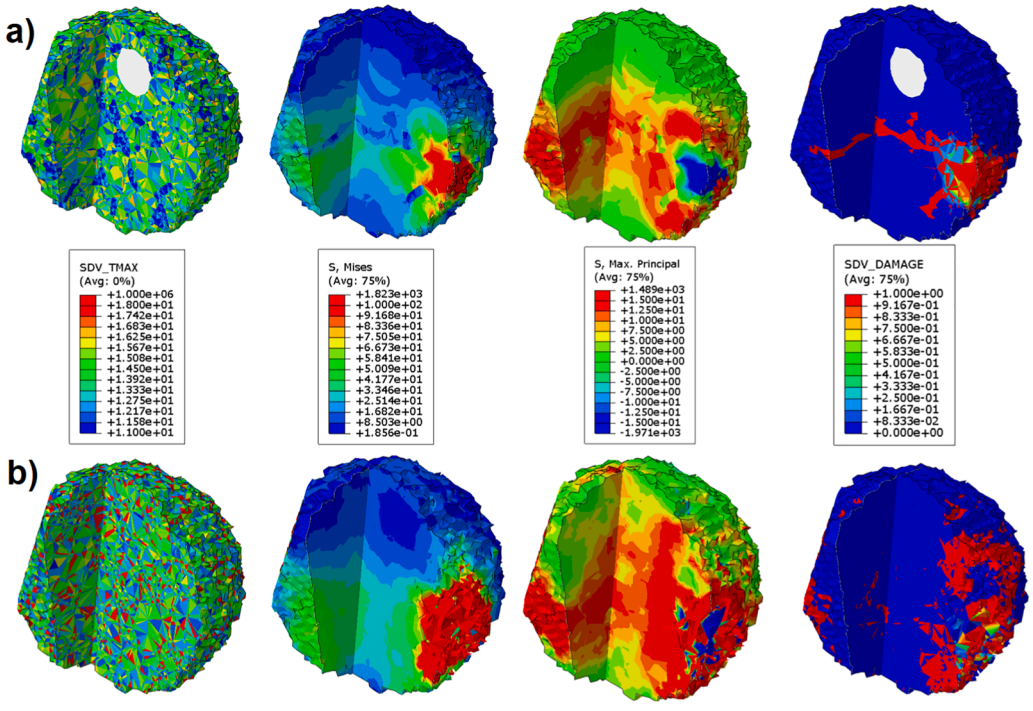


**Fig. 10.** Synthetic heterogeneous (a) and homogenized (b) slag particles during crushing, showing tensile strength distributions, equivalent stress, maximum principal stress, and damage contours after first dominant failure propagation.

works (Lindroos et al., 2015).

To narrow the gap between jaw material microstructural scale and macroscale mineral-jaw contacts, a loading history transfer procedure is performed. In the present case, simplified loading histories are obtained from the jaw crushing simulations from the contact zones. Only surface pressure is transferred to the microscale model representing jaw material, while omitting the shear and surface slip tractions.

Fig. 11b shows the polycrystal aggregate and the loading sequence with surface pressure. A polycrystal microstructure with 250 grains were used to describe Hadfield material. Two cases were investigated, one with a constant surface pressure over the microstructure and the second one with concentrated pressure on the aggregate. Fig. 11a shows a surface pressure evolution in one contact zone in the jaw crusher simulations for the heterogeneous slag. Similar loading history was imposed to the microstructural RVEs (medium). A second loading was included to investigate more severe loading scenario (hard).

Hadfield steels are strain rate sensitive materials that endure notable increase in strength at high strain rates (Lindroos et al., 2018). The dynamic nature of mineral crushing subjects high strain rate conditions to the surface deformation of jaw materials, as pointed out. Accordingly, two scenarios were investigated with a dynamic strain rate case derived from the loading history of the currently simulated jaw crushing incident and a lower strain rate case with a thousand times longer time period for the loading. Fig. 12 shows the stress–strain response of the jaw material, cumulative plastic shear generated by dislocation slip and deformation twinning, and total twin volume fraction crucial to materials hardening capability, at two strain rates and with two surface pressure loads over the whole aggregate.

A notable strain rate dependency is observed for the material. The lower surface pressure of 560 MPa generates approximately ten times larger axial strain to the aggregate than the dynamic strain rate. This behavior is related to dynamic strength of the material. A quasi-static macroscopic yield strength of the investigated Hadfield steel is about 480 MPa at strain rate of $0.001\,s^{-1}$, whereas the apparent yield strength increases approximately to 800 MPa at $4000\,s^{-1}$ (Lindroos et al., 2018). Therefore, the increase in dynamic materials behavior residues only minor microplasticity in the material with 560 MPa surface loading. Both strain rate regimes experience small rachetting like behavior with saturating type of plastic increment as a consequence of the uniaxial cyclic loading.

Larger 800 MPa loading causes heavy plasticity during the first loading cycle, which can from tribological perspective to be understood as increased surface hardness due to notable strain hardening of the material. The deformation experienced during the first cycle at the low strain rate causes the material harden so dramatically that the subsequent cycles cause only minor plasticity. Plasticity at high strain rate condition is more limited during the first cycle and the subsequent load cycles also increase overall plastic strain. However, a saturation type of behavior is observed rapidly after about five cycles. One relevant reason for this behavior is the promoted twin initiation and growth in the material at a high strain rate, which strongly increases the material's flow stress, i.e., the twin volume fraction increases faster at high strain rate with respect to the axial strain.

Fig. 13 demonstrates the material strengthening after 560 and 800 MPa constant pressure loading. To demonstrate the effectiveness of the pre-cyclic deformation to material flow stress, a tensile test is performed at a low strain rate of $0.1\,s^{-1}$ after cyclic deformation. The ten cycle dynamic loading of 560 MPa has hardly increased the material flow stress (or hardness) in compared to bulk state as-cast material. More drastic increase is observed after cyclic dynamic loading at 800 MPa. Material's uniaxial flow stress increases from about 480 MPa to 635 MPa, indicating an increase of about 30%.

Fig. 13 c,d show the residual equivalent stress distribution and cumulative plastic shear generated by dislocation slip and deformation twinning, respectively, after ten cycles of 800 MPa loading. The grain structure exhibits typical orientation dependent soft and hard grain deformation behavior with plastic localization in some grains. Due to polarized nature of deformation twinning, twin favorable orientations generated more deformation twins and other grains deform mainly by slip, which together successively strengthens the material during cyclic loading. Fig. 13 e-h present a special case with concentrated surface loading of 800 MPa and 1200 MPa. The simplified loading is aimed to mimic localized surface pressure contact on the Hadfield jaw material. The lower 800 MPa load generates expected plasticity in close-vicinity of the surface loading. Higher 1200 MPa load induces notably larger stress affected zone around the loaded zone with greater plastic strain concentrations. The flow stress or hardness of the heavily deformed region has increased notably. The near vicinity grains, in turn, are not affect that greatly. This obviously suggests that the single abrasive contacts cause hardening only in the limited vicinity indenting/contact zone and the overall surface hardening process requires large amount of contacts. However, it is worth noting that the subsurface grains are already triggering dislocation slip and twinning during the process. Then the evolution of surface material wear reveals already hardened surface below.

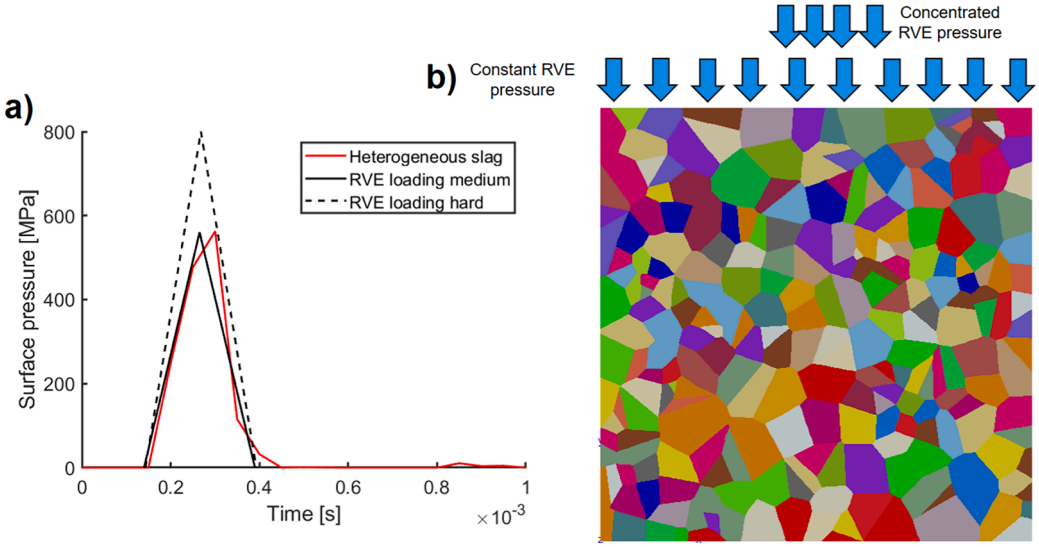


**Fig. 11.** a) Surface pressure inputs for crystal plasticity model with extracted surface load from jaw crusher and two synthetic loading scenarios, b) polycrystalline microstructural aggregate loaded with surface pressure.

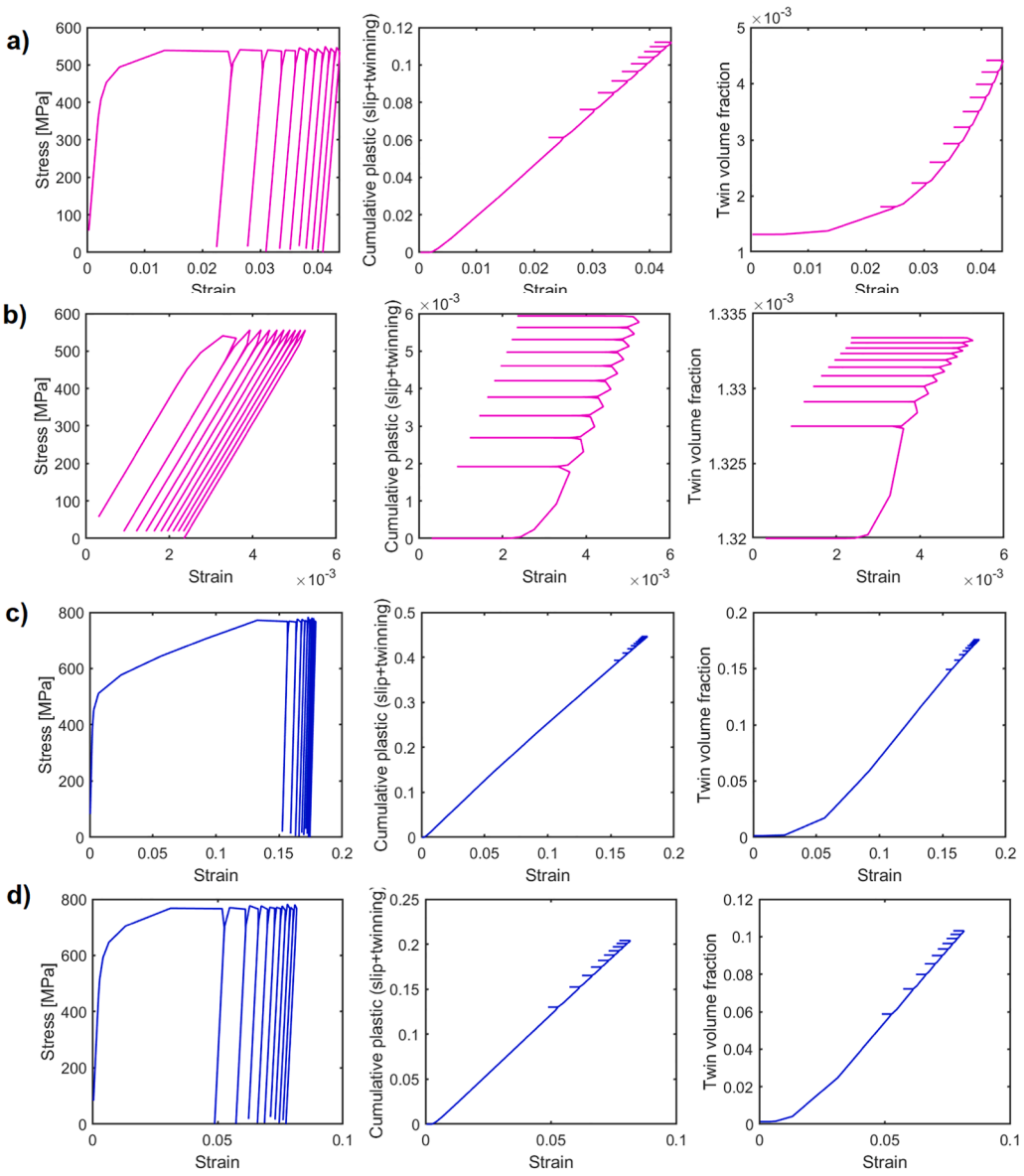


**Fig. 12.** Polycrystal level averaged responses of stress–strain evolution, cumulative plastic strain (slip + twinning), and evolution of twin volume fraction for a) quasi-static strain rate loading at surface pressure of 560 MPa, b) dynamic strain rate loading at surface pressure of 560 MPa, c) quasi-static strain rate loading at surface pressure of 800 MPa, d) dynamic strain rate loading at surface pressure of 800 MPa.

The present simulation technique can address the overall evolution of material hardening during crushing process as long as the subjected mineral type dependent surface loads are physically relevant and realistic.

## 4. Discussion

The multi-scale linkage between microstructure and macroscale material behavior offers a possibility to incorporate strength and fracture model sensitive to microstructural characteristics. The methodology allows to use the data from conventional and advanced characterization techniques on phase specific level and homogenize the material behavior to more convenient use in macroscopic scale. The present approach uses the same material model for strength and damage on microscale and macroscale with interdependent model parametrization. The core of the present method relies much on the various techniques defining phase specific mechanical properties, such as micro- and nanoindentation techniques. The estimation based parametrization using hardness and fracture toughness values could be improved with advanced characterization method, such as in situ nanopilar experiments inside and at the interfacial regions (Lunt et al., 2015). Slag also contains certain amount of internal cracks that could be introduced in the model, however, their distribution and characteritics need to be defined properly to improve the model's prediction capability and not actually decrease it because of unrealistic setting in the microstructure. Nevertheless, present work focuses much on providing efficient way to approximate macroscale material model parameters using microscale information to be able to generate robust multi-scale workflow for typical numerical solvers dealing with plasticity and damage in engineering, e.g., FEM and DEM.

In general, it is worth noting that the method does not exactly place constraints on using different more detailed physics based micromechanical models at the microstructural level. One possible way is to imitate crystal plasticity models and use crystalline level fracture models, such as suggested in (Lindroos et al., 2019), to estimate phase specific properties based on crystalline structure and their susceptibility to brittle type cleavage fracture. In addition, non-local model extensions can attribute length-scale effects and regularization of damage

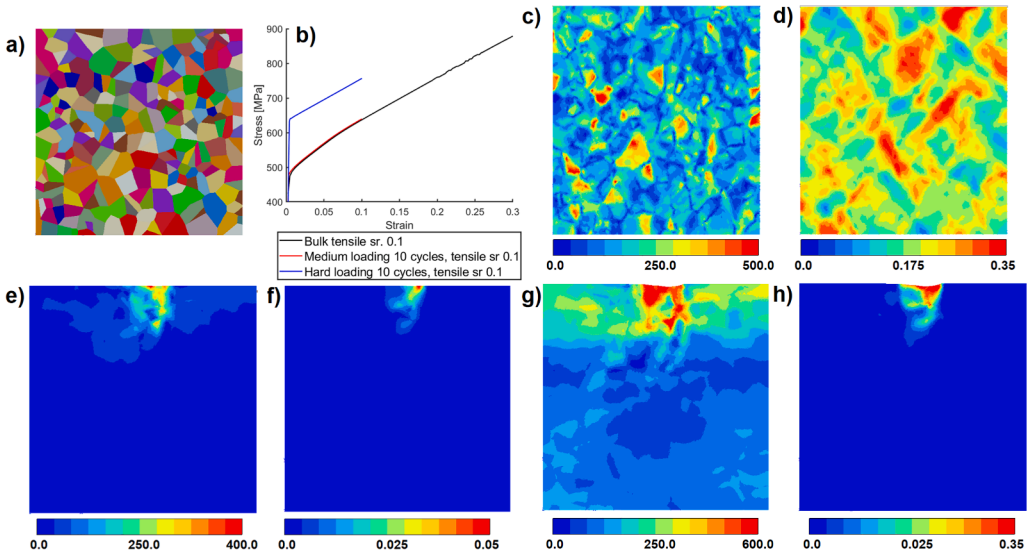


**Fig. 13.** a) Computational microstructure of Hadfield steel, b) stress–strain tensile curves of bulk as-cast material and two pre-deformed material states with cyclic loading extended with a tensile loading, c),e),g) residual Von Mises stress contour, and d),f),h) cumulative plastic shear (slip + twinning) after ten load cycles. In c-d) the microstructure is loaded with 800 MPa constant pressure, e-f) the microstructure is loaded with 800 MPa on a concentrated zone in the middle, and g)-h) with 1200 MPa pressure loading on a concentrated zone.

preceeding plastic localization (Rattez et al., 2018). Micromechanical models can provide a deformation response to representative volume elements defining the microstructure, as for example is presented in Figs. 3, 5. The RVE could be loaded in various different ways to provide virtual stress–strain curves, strain rate dependent data, and confinement pressure dependent data for any given macroscopic strength and fracture model. With the presently investigated slag material, using crystal plasticity based model is only one part of the possible solution since some of the phases are amorphous or only partly crystalline, that require different approaches in general (Schuh et al., 2007).

The single particle jaw crushing simulations showed that strictly element based selection of material properties and distributions can elevate heterogeneity that exists in various rocks and slag materials, as was observed in Figs. 6, 7. However, the prediction capability of this homogenization choice is somewhat limited to small internal changes of material properties. For example, only a small difference was observed with slag material containing 5% or 10% of manganese inclusions. On one hand, the result is partly contributed by the arbitrary shape of the crusher particle that generated high stress concentrations in contact conditions with the jaws. On the other hand, the strict element based approach with distinction to matrix phase and manganese inclusion phase does not necessarily provide enough sensitivity in the present case, at least with small realistic volume fractions of inclusions. A second option is to homogenize the whole particle as one phase with large variations of material properties based on microstructure scale results with the expense of local accuracy. Both of the options are computationally efficient in terms of simulating large number of crushed particles. Besides the conventional mesh refinement techniques, various finite element framework related improvements can be applied, such as (Saksala et al., 2015). These model extensions concentrate in providing more detailed crack behavior again at the expense of computational effort. The justification of these type of approach is their potential capability to more accurate crack path evolution during crushing that could be used to benefit estimations of end product quality, e.g., an important aspect in selective comminution. Crushing forces, closely related to energy dissipation of the process (Terva et al., 2018), could also be increased/decreased by more detailed damage approaches to a certain extent. In addition, the accuracy of computational contact discretization gains importance when the micromechanical modeling of the counter-surface is a matter of interest. However, given high-throughput perspective of the present work, high computational cost easily then make many of the detailed methods unattractive as engineering tools.

Discretization of slag particle with the identified most dominant phases is an effective method to treat necessary heterogeneities in the material. The use discretization in Fig. 8 and related fracture response in Figs. 9, 10 does not intensively increase the computational cost of the method whenever the phase-to-phase does not require extremely detailed meshing. Instead, the behavior of slag was markedly changed in the simulations. Heterogeneity arising from the mixed phase matrix and inclusion or pore defects act as weak discontinuities that elevate local stresses and often promote fracture. The general observation related to damage networks in Fig. 10 suggest the heterogeneous discretization provides more realistic fracture patterns with few dominant cracks, while the investigated homogenized slag particle has a tendency to behave like a second phase strengthened material exhibiting large number of dense and eventually connecting crack networks. The cost-to-detail trade-off between the two discretizations is then clear and thus can affect the end result notably because of the homogenized smoothing. The ultimate case of adding scatter/details in the single phase matrix parametrization of the homogenized approach and providing more definite larger manganese phase inclusions beyond single element sized precipitates would, in fact, resemble the full multiphase discretization model of Fig. 8a.

Wear parts of crushing equipment are in relevant role when accessing the overall efficiency of the process in terms of premature wear and imprecise worn geometries that affect end product quality. Macroscopic level plasticity models may be used to estimate the deformation response of materials at application level. Incorporation of wear may be performed to establish lifetime estimates of the material solution. However, in-depth models are required to parametrize any macroscopic and global level phenomenological wear models that in many cases use common load inputs related tribological contacts, such as contact pressures, material hardness, and friction. Micromechanical modeling approach is suitable in providing necessary information of local plasticity and damage susceptibility of the material with a viable link to the materials microstructure. Two common choices are often made to accomplish scale transition from macroscale to microscale. Direct method reduces model scale down to a level of single abrasive contacts (Lindroos et al., 2019) or detailed contact between rough surfaces (Durand et al., 2014), which are computationally expensive choices when estimating deformation and damage responses. An indirect approach used in this work allows to simplify contact conditions to load based scenario, in which the surface loads are transferred to microstructural level using submodeling ideology. This choice makes the computations more affordable and large amount of data can be generated more easily. An additional benefit arising from micromechanical modeling is that the developments towards being able to predict wear are better transferable than classical wear modeling, i.e., as

microstructural features are directly included rather than in classical methods (see, for example, (Laukkanen et al., 2020), where a similar approach has been exploited for wear prediction).

Two main observations could be made based on the crystal plasticity simulations with the load transfer models. The model using constant surface pressure over the whole aggregate size can be used to analyze the microstructures capability to harden under arbitrary loading setting, providing a general view on the deformation response of large number of grains or microstructural features. Damage approach was omitted in the present context for simplicity, however, a large number of various intra-grain and inter-grain within RVE deformation responses can statistically be used to sample materials susceptibility to develop damage sites. Furthermore, the RVE level homogenized results may be used to estimate materials hardening behavior responsible of evolution of surface hardness, which is an ingredient of many phenomenological wear formulations for metals.

An approach to concentrate surface loading on limited surface area of the RVE yields information about the loading bearing and hardening capability of near surface grains. Plastic strain localization and stress concentrations can be analyzed in the surface region and direct crystalline level damage constitutes are applicable to predict formation of cracks that lead to release of wear particles (Lindroos et al., 2019). Alternatively, material level performance indicators may be used to analyze susceptibility to microstructure level damage, which often make use of the inputs related to plastic shear and local stresses, e.g., fatigue indicator parameters (Pinomaa et al., 2019; Schäfer et al., 2019). Wear rate may then be formulated based on the microstructure level response of the material with respect to arbitrary loading scenarios. However, statistically relevant information require large amount of cases to be investigated and relatively large amount of load cycles are needed to establish certain wear rates based on the micromechanical approach. In spite of the demanding computational framework of crystal plasticity models, especially for advanced constitutive models, the computational cost is still not necessarily overwhelming when the load is subjected with a load transfer method.

## 5. Conclusions

A multi-scale modeling methodology was proposed for investigating the fracture behavior and significance of micromechanical modeling in the crushing process of manganese containing slag material. The following main observations and conclusions were made.

- Multi-scale workflow is established for manganese containing slag material utilizing finite element method. Microstructure based models involving phase specific material properties is usable in terms of parametrizing phenomenological fracture models at macroscopic scale, either being homogenized or phase-specific models. The role of valid computational workflow is significant when focusing to optimize the comminution process that depends on crushable medium heterogeneity.
- Phase specific macroscopic fracture model provides more detailed level fracture patterning than homogenized material model. The microstructure based model allows more direct sensitivity analysis of the effects of different phases and their mechanical contribution to fracture process with only a marginal increase in computational cost.
- Phase-to-phase discretization of the most dominant phases provides more natural fracture behavior than element-wise distribution of material properties to matrix and inclusion phases. Homogenization of the overall material properties into single phased material with high property variation is a plausible approach in addition to direct dominant phase-to-phase approach.
- Crystal plasticity method is a vital piece of the multi-scale workflow to investigate and analyze deformation, hardening and ultimately provide wear related estimates of metallic wear parts. Load transfer from macromodel to microscale model is efficient way to avoid computational cost of discretized fine scale abrasive-impact contacts. A two way coupling that transfer surface hardening potential of the material back to macroscale is possible with the suggested framework.

## Declaration of Competing Interest

The authors declare that they have no known competing financial interests or personal relationships that could have appeared to influence the work reported in this paper.

## Acknowledgements

This work was supported by EIT Raw Materials "GREENY", Grinding Energy Efficiency, upscaling project Grant No. 18009.

## References

Hesse, M., Popov, O., Lieberwirth, H., 2017. Increasing efficiency by selective comminution. Miner. Eng. 103–104, 112–126. https://doi.org/10.1016/j.mineng.2016.09.003.

Leon, L.G., Johan Hogmalm, K., Bengtsson, Magnus, 2020. Understanding Mineral Liberation during Crushing.

Terva, J., Valtonen, K., Siitonen, P., Kuokkala, V.-T., 2020. Correlation of wear and work in dual pivoted jaw crusher tests. Journal of Engineering Tribology 234, 334–349. https://doi.org/10.1177/1350650118795566.

Ulsen, C., Tseng, E., Angulo, S.C., Landmann, M., Contessotto, R., Balbo, J.T., Kahn, H., 2019. Concrete aggregates properties crushed by jaw and impact secondary crushing. Journal of Materials Research and Technology. https://doi.org/10.1016/j.jmrt.2018.04.008.

Da Cunha, E.R., De Carvalho, R.M., Tavares, L.M., 2013. Simulation of solids flow and energy transfer in a vertical shaft impact crusher using DEM. Miner. Eng. 43–44, 85–90. https://doi.org/10.1016/j.mineng.2012.09.003.

Djordjevic, N., Shi, F.N., Morrison, R.D., 2003. Applying discrete element modelling to vertical and horizontal shaft impact crushers. Miner. Eng. 16, 983–991. https://doi.org/10.1016/j.mineng.2003.08.007.

Jonsén, P., Pålsson, B., Stener, J., Hägglund, H-., 2014. A novel method for modelling of interactions between pulp, charge and mill structure in tumbling mills. Miner. Eng. 63, 65–72.

Jonsén, P., Stener, J., Pålsson, B., Hägglund, H-., 2015. Validation of a model for physical interactions between pulp, charge and mill structure in tumbling mills. Miner. Eng. 73, 77–84.

Jonsén, P., Hammaberg, S., Pålsson, B., Lindkvist, G., 2019. Preliminary validation of a new way to model physical interactions between pulp, charge and mill structure in tumbling mills. Miner. Eng. 130, 76–84.

Larsson, S., Pålsson, B., Paria, M., Jonsén, P., 2020. A novel approach for modelling of physical interactions between slurry, grinding media and mill structure in stirred media mills. Miner. Eng. 138, 106180.

Lindroos, M., Laukkanen, A., Andersson, T., 2019. Micromechanical modeling of polycrystalline high manganese austenitic steel subjected to abrasive contact. Friction 10, 1237.

Holmberg, K., Laukkanen, A., Turunen, E., Laitinen, T., 2014. Wear resistance optimisation of composite coatings by computational microstructural modelling. Surf. Coat. Technol. 247, 1–13.

Holmberg, K., Laukkanen, A., Ghabchi, A., Rombouts, M., Turunen, E., Waudby, R., Suhonen, T., Valtonen, K., Sarlin, E., 2014. Computational modelling based wear resistance analysis of thick composite coatings. Tribol. Int. 72, 13–30.

Desrues, J., Argilaga, A., Caillerie, D., Combe, G., Nguyen, T., Richefeu, V., Dal Pont, S., 2019. From discrete to continuum modelling of boundary value problems in geomechanics: An integrated fem-dem approach. International Journal of numerical and analytical methods in geomechanics 43, 919–955.

Liu, X., Han, G., Wang, E., Wang, S., Nawnit, K., 2018. Multiscale hierarchical analysis of rock mass and prediction of its mechanical and hydraulic properties. Journal of Rock Mechanics and Geotechnical Engineering 10, 694–702.

Golshani, A., Okui, Y., Oda, T., Takemura, M., 2006. A micromechanical model for brittle failure of rock and its relation to crack growth observed in triaxial compression tests of granite. Mech. Mater. 38, 287–303.

Xie, N., Zhu, Q.-Z., Shao, J.-F., Xu, L.-H., 2012. Micromechanical analysis of damage in saturated quasi brittle materials. Int. J. Solids Struct. 49, 919–928.

Zhang, Y., Wong, L., Chan, K., 2018. An extended grain-based model accounting for microstructures in rock deformation. Journal of Geophysical Research: Solid Earth 124, 125–148.

Sun, H., Gao, Y., Zheng, X., Chen, Y., Jiang, Z., Zhang, Z., 2019. Meso-scale simulation of concrete uniaxial behavior based on numerical modeling of ct images. Materials 12, 3403.

W. Zhou, X. Ji, M.G., Y. Chen, Fdem simulation of rocks with microstructure generated by voronoi grain-based model with particle growth, Rock Mechanics and Rock Engineering 53 (2019) 1909–1921.

Li, X., Zhang, S., Yan, E.-C., Shu, D., Cao, Y., Li, H., Wang, S., He, Y., 2017. An Analysis of the Mechanical Characteristics and Constitutive Relation of Cemented Mercury Slag. https://doi.org/10.1155/2017/3573012.

Tang, Z., Hu, Y., Tam, V.W., Li, W., 2019. Uniaxial compressive behaviors of fly ash/slag-based geopolymeric concrete with recycled aggregates. Cement and Concrete Composites 104, 103375. https://doi.org/10.1016/j.cemconcomp.2019.103375.
Lindroos, M., Cailletaud, G., Laukkanen, A., Kuokkala, V.-T., 2018. Crystal plasticity modeling and characterization of the deformation twinning and strain hardening in had?eld steels. Mater. Sci. Eng., A 720, 145–159.
Lindroos, M., Laukkanen, A., Cailletaud, G., Kuokkala, V.-T., 2018. Microstructure based modeling of the strain rate history effect in wear resistant hadfield steels. Wear 396–397, 56–66.
Lindroos, M., Apostol, M., Heino, V., Valtonen, K., Laukkanen, A., Holmberg, K., Kuokkala, V.-T., 2015. The deformation, strain hardening, and wear behavior of chromium-alloyed had?eld steel in abrasive and impact conditions. Tribology letters 57, 1–11.
H. Apazablanco, C. Carvajal, H. Lieberwirth, Grinding energy efficiency, the greeny project, 2020. To be published.
M. Hokka, J. Black, D. Tkalich, M. Fourmeau, A. Kane, N.-H. Hoang, C. Li, K.V.-T. Chen, W.W., Effects of strain rate and con?ning pressure on the compressive behavior of kuru granite, International journal of impact engineering 91 (2016) 183–193.
Fourmeau, M., Kane, A., Hokka, M., 2017. Experimental and numerical study of drill bit drop tests on kuru granite. Philosophical Transactions A 375, 20160176.
Johnson, G., Holmquist, T., 1994. An improved computational constitutive model for brittle materials. AIP Conf. Proc. 309, 981–984.
Sakala, T., Hokka, M., Kuokkala, V.-T., 2017. Numerical 3d modeling of the effects of strain rate and confining pressure on the compressive behavior of kuru granite. Computer and Geotechnics 88, 1–8.
Zhang, Z., 2002. An empirical relation between mode i fracture toughness and the tensile strength of rock. Int. J. Rock Mech. Min. Sci. 39, 401–406.
Feng, G., Wang, X.-C., Kang, Y., Luo, S.-G., Hu, Y.-Q., 2019. An empirical relation between mode i fracture toughness and the tensile strength of rock. Applied Sciences 9, 1326.
Kahraman, S., Fener, M., Kozman, E., 2012. Predicting the compressive and tensile strength of rocks from indentation hardness index. The Journal of The Southern African Institute of Mining and Metallurgy 112, 331–339.
Zavacky, M., Stefanak, J., Horak, V., Mica, L., 2017. Statistical estimate of uniaxial compressive strength of rock based on shore hardness. Procedia Engineering 191, 248–255.
Mardoukhi, A., Saksala, T., Hokka, M., Kuokkala, V.-T., 2017. A numerical and experimental study on the tensile behavior of plasma shocked granite under dynamic loading. Rakenteiden mekaniikka 50, 41–62.
Laukkanen, A., Pinomaa, T., Holmberg, K., Andersson, T., 2016. Effective interface model for design and tailoring of WC–Co microstructures. Powder Metall. 59, 20–30.
Lunt, A., Mohanty, G., Neo, J., Michler, T.K., Korsunsky, A., 2015. Microscale resolution fracture toughness profiling at the zirconia-porcelain interface in dental prosthesess, Proc. SPIE 9668. Micro+Nano Materials, Devices, and Systems 101, 96685S.
Lindroos, M., Laukkanen, A., Andersson, T., Vaara, J., Mantyla, A., Frondelius, T., 2019. Micromechanical modeling of short crack nucleation and growth in high cycle fatigue of martensitic microstructures. Comput. Mater. Sci. 170, 109185.
Rattez, H., Stefanou, I., Sulem, J., Vevekakis, M., Poulet, T., 2018. Numerical analysis of strain localization in rocks with thermo-hydro-mechanical couplings using cosserat continuum. Rock Mech. Rock Eng. 51, 3295–3311.
Schuh, C., Hufnagel, T., Ramamurty, U., 2007. Mechanical behavior of amorphous alloys. Acta Mater. 55, 4067–4109.
Saksala, T., Brancherie, D., Harari, I., Ibrahimbegovic, A., 2015. Combined continuum damage-embedded discontinuity model for explicit dynamic fracture analyses of quasi-brittle materials. Numerical Methods in Engineering 101, 230–250.
Terva, J., Kuokkala, V.-T., Valtonen, K., Siitonen, P., 2018. Effects of compression and sliding on the wear and energy consumption in mineral crushing. Wear 398–399, 116–126.
Durand, J., Proudhon, H., Cailletaud, G., 2014. Contact between rough surfaces: Crystal plasticity influence on the contact tightness estimation. Blucher Mechanical Engineering Proceedings 1, 1–12.
Laukkanen, A., Lindgren, M., Andersson, T., Pinomaa, T., Lindroos, M., 2020. Development and validation of coupled erosion-corrosion model for wear resistant steels in environments with varying ph. Tribol. Int. 151, 106534. https://doi.org/10.1016/j.triboint.2020.106534 https://www.sciencedirect.com/science/article/pii/S0301679X20303662.
Pinomaa, T., Yaschuk, I., Lindroos, M., Andersson, T., Provatas, N., Laukkanen, A., 2019. Process-structure-properties-performance modeling for selective laser melting. Metals 9, 1138.
Schäfer, B., Sonnweber-Ribic, P., Hassan, H., Hartmaier, A., 2019. Micromechanical modelling of the influence of strain ratio on fatigue crack initiaion in a martensitic steel - a comparison of different fatigue indicator parameters. Materials 12, 2852.